Single-Molecule Magnets

International Edition: DOI: 10.1002/anie.201904645
German Edition: DOI: 10.1002/ange.201904645

Strong Exchange Couplings Drastically Slow Down Magnetization Relaxation in an Air-Stable Cobalt(II)-Radical Single-Molecule Magnet (SMM)

Uta Albold[+], Heiko Bamberger[+], Philipp P. Hallmen, Joris van Slageren, and Biprajit Sarkar**

Abstract: *The energy barrier leading to magnetic bistability in molecular clusters is determined by the magnetic anisotropy of the cluster constituents. By incorporating a highly anisotropic four-coordinate cobalt(II) building block into a strongly coupled fully air- and moisture-stable three-spin system, it proved possible to suppress under-barrier Raman processes leading to 350-fold increase of magnetization relaxation time and pronounced hysteresis. Relaxation times of up to 9 hours at low temperatures were found.*

Research into molecular materials that display magnetic bistability of purely molecular origin has been pursued since the discovery of slow relaxation of the magnetization in a Mn_{12} cluster.[1] Magnetic bistability derives from the presence of an energy barrier between up- and down-orientations of the magnetic moment. Because in a first approximation, the energy barrier is proportional to the square of the ground-state spin-quantum number S ($\Delta E = DS^2$), many efforts were directed to increasing this value.[2] Later it was realized that with increasing spin, the zero-field splitting constant D decreases, leading to little increase of the energy barrier.[3] The constant D of a spin state is a linear combination of the single-ion zero-field splittings.[4] This realization sparked research into developing systems with larger single-ion anisotropies. Currently, the best performing systems are dysprosocenium,[5–7] and low-coordinate transition-metal ions.[8,9] An example of the latter is provided by four-coordinate cobalt(II) complexes.[10] These cobalt systems have the distinct advantage in that they are not air sensitive, in contrast to low-coordinate dysprosium and other transition-metal complexes. Although large energy barriers have been reported for four-coordinate cobalt(II) complexes, no true bistability, as indicated by substantial coercivity in the magnetic hysteresis curve without zero-field step, has been reported as yet. One of the reasons for lack of coercivity is the occurrence of under-barrier relaxation processes, such as the Raman process or quantum tunneling of the magnetization.[11] Such processes are expected to be suppressed in strongly exchange coupled multi-spin systems. A good example of this is given by radical bridged dinuclear lanthanide complexes.[12–14] The disadvantage of lanthanides in this regard is that truly strong exchange couplings are exceedingly challenging to achieve. Such very strong couplings are required, because moderate exchange couplings will give rise to exchange coupled multiplets below the energy levels arising from the single-ion anisotropy. These multiplets can function as intermediate states in an Orbach relaxation process, thus effectively short-cutting the energy barrier. Such very strong exchange couplings can be more easily achieved in transition-metal-radical systems, in which coupling strengths of hundreds of cm^{-1} have been reported.[15–17]

With these thoughts in mind, we set out to use the $[Co^{II}(L_A^{2-})_2]^{2-}$ (H_2L_A is 1,2-bis(methanesulfonamido)benzene) complex (**1**) as an inspiration in a multispin metal-radical complex (Figure 1). We have recently shown that this complex possesses a D value in excess of 100 cm^{-1}, separating the two Kramers doublets of the $S = 3/2$ by more than 200 cm^{-1}.[10] Herein we present the synthesis as well as theoretical and magnetic investigations of air-stable radical-bridged $(K\text{-}18\text{-}c\text{-}6)_3[\{(H_2L_B^{2-})Co^{II}\}_2(\mu\text{-}L_B^{3\cdot-})]$ (**2**, $H_4L_B =$

[*] M. Sc. U. Albold,[+] Prof. Dr. B. Sarkar
Institut für Chemie und Biochemie
Freie Universität Berlin
Fabeckstrasse 34–36, 14195 Berlin (Germany)
E-mail: Biprajit.Sarkar@fu-berlin.de
M. Sc. H. Bamberger,[+] M. Sc. P. P. Hallmen, Prof. Dr. J. van Slageren
Institut für Physikalische Chemie
Universität Stuttgart
Pfaffenwaldring 55, 70569 Stuttgart (Germany)
E-mail: slageren@ipc.uni-stuttgart.de
[+] These authors contributed equally to this work.
Supporting information and the ORCID identification number(s) for the author(s) of this article can be found under: https://doi.org/10.1002/anie.201904645.

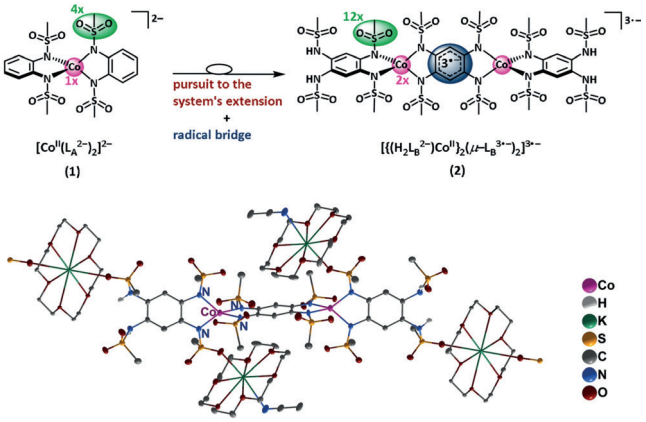

Figure 1. Top: Schematic representation of the complexes. Bottom: Single-crystal ORTEP view of **2** in the polymeric chain of the crystal. Ellipsoids of **2**/K-18-c-3 shown at 50%/20% probability level. H atoms (except for NH groups) omitted for clarity.[31]

1,2,4,5-tetrakis(methanesulfonamido)benzene). In particular, we show that in this strongly coupled multispin system, Raman relaxation has been strongly suppressed leading to a slowing down of the relaxation of the magnetization by up to 350 times compared to rates found for the mononuclear building block **1**.

Complex **2** was synthesized by the partial and complete deprotonation of the ligand H_4L_B with KO^{t}Bu in the presence of 18-crown-6 in MeCN at room temperature, subsequent addition of $Co(BF_4)_2{\cdot}6H_2O$ and oxidation with pure oxygen. Its molecular structure was determined by single-crystal X-ray crystallography (Figure 1). Compound **2** crystallizes in the monoclinic space group $P2(1)/c$ (Table S1 in the Supporting Information) with two distorted tetrahedral coordinated cobalt(II) centers and a center of inversion located at the middle of the complex. The ancillary ligands are perpendicularly oriented to the bridging ligand, which displays shorter C–N bonds than the ancillary ligands (Table S2). The cobalt–ligand bond lengths and the bond angles and distortions at the cobalt centers are virtually identical in **1** and **2** (Table S3). In fact, using the coordination polyhedron of **1** as a reference, a distortion value of only 0.014 is found using the SHAPE geometry analysis programme.[18] Complex **2** crystallizes with four 18-crown-6 encased potassium counterions, two located on either side of the molecule and two are shared, connecting the complexes to a polymeric chain (Figure S1). Hence, three whole counterions can be assigned to one molecule. These structural features demonstrate that the bridging tetra-aza ligand is triply negatively charged and therefore contains an unpaired electron. In spite of the open shell nature of the bridge, the complex as such is completely air- and moisture stable in the solid-state and in solution, pointing to the unique nature of this radical bridge.

To assess the strength and nature of the magnetic couplings of the cobalt(II)-radical-cobalt(II) system **2**, as well as to investigate its zero-field splitting, magnetic susceptibility measurements were carried out (Figure 2).

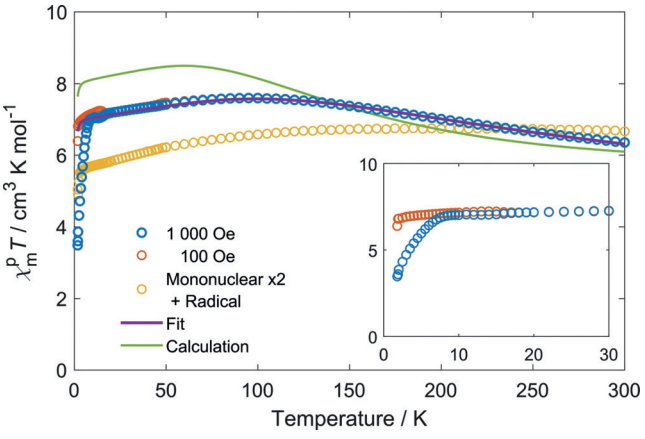

Figure 2. Susceptibility temperature product (χT) as a function of temperature for a pressed powder pellet sample of **2** in applied field of 0.1 T (blue symbols), as well as a fit using parameters given in the text (red line) and the ab initio-calculated susceptibility (green line). The yellow symbols indicate twice the χT value of **1**[10] plus a 0.375 cm^3 K mol^{-1} contribution for the radical. The inset magnifies the low-temperature region.

The room temperature χT value of 6.36 cm^3 K mol^{-1} is rather close to what is expected for non-interacting cobalt ions and one radical spin ($\chi T = 2{\cdot}(2.48^2/8){\cdot}3/2{\cdot}5/2 + 0.5{\cdot}1/2{\cdot}3/2 = 6.14$ cm^3 K mol^{-1}, where the average g-value for **1**[10] has been used), in spite of the expected strong zero-field splitting and exchange interactions. On lowering the temperature, the χT product increases, reaches a maximum of 7.6 cm^3 K mol^{-1} at 100 K and subsequently decreases slowly before dropping precipitously at around 10 K. Measurements at smaller applied fields reveal a less precipitous drop of χT at the lowest temperatures. This is a first indication for the fact that the magnetic moment is not in thermal equilibrium with its surroundings and thus a first indication for slow relaxation of magnetization. The data are qualitatively similar to what was found for the monomeric complex **1**. Quantitatively, the χT values around room temperature for **2** (6.31 cm^3 K mol^{-1} at 300 K) are lower than twice the value for **1** plus 0.375 cm^3 K mol^{-1} for the radical center (6.66 cm^3 K mol^{-1}), which is consistent with antiferromagnetic exchange. The significantly higher χT of **2** at low temperatures suggests a ferrimagnetic high-spin ground state. The χT data can be very well fitted on the basis of the following spin Hamiltonian [Eq. (1)]:

$$\mathcal{H} = \sum_{i=1}^{2} J_{\mathrm{Co-Rad}} \hat{\vec{S}}_{\mathrm{Co},i} \cdot \hat{\vec{S}}_{\mathrm{Rad}} + D_{\mathrm{Co},i} \hat{S}_{z,i}^2 + \mu_B \vec{B} \cdot \underline{g}_{\mathrm{Co},i} \cdot \hat{\vec{S}}_{\mathrm{Co},i} + g_{\mathrm{Rad}} \mu_B B \hat{\vec{S}}_{\mathrm{Rad}} \quad (1)$$

The best fit yields the values $J_{\mathrm{Co-Rad}} = 440(40)$ cm^{-1}, $D_{\mathrm{Co}} = -115(15)$ cm^{-1}, $g_{\mathrm{Co},\parallel} = 2.85(3)$, $g_{\mathrm{Co},\perp} = 2.09(7)$. These values confirm both the antiferromagnetic nature of the exchange coupling and the ferrimagnetic, high-spin ground state.

To obtain more information on the values of D and J, we carried out multireference ab initio calculations. However, such methods currently cannot easily tackle a molecule of the size of **2** with three open shell centers. Therefore, in a first step we replaced one of the cobalt ions by diamagnetic zinc(II). Furthermore, we forced the bridging ligand to be closed shell by adding one electron. The orbitals resulting from a LDF-CAHF-calculation[19] on this fictitious compound were used as a starting approximation for a subsequent calculation, where one electron was again removed from the bridging ligand HOMO giving an open-shell ligand. Using an active space consisting of the five cobalt d-orbitals, as well as the bridging-ligand frontier orbitals (two π- and two π*-orbitals), that is, CAS(10,9)), we carried out a SA-CASSCF calculation of this system with two open shells, calculating 10 quintet and 10 triplet roots. Description of the zero-field splitting requires taking into account spin-orbit coupling, while superexchange interactions involve dynamical correlations. Spin-orbit coupling was dealt with by constructing the matrix of the Breit-Pauli spin-orbit operator (in the atomic mean-field approximation). The energies of the diagonal elements were replaced by those calculated at the multi-state CASPT2 level, which takes into account dynamical correlations. Diagonalization of this matrix gave the final states. The lowest states were projected onto a $(S = 3/2)-(S = 1/2)$ dimer spin Hamiltonian analogous to Equation (1). This allows

extracting spin Hamiltonian parameter values as $J_{Co\text{–}Rad} = 174\ cm^{-1}$ and $D_{Co} = -110\ cm^{-1}$. The D_{Co} value is very close to the value obtained from fitting the susceptibility. The $J_{Co\text{–}Rad}$ value is less than half of what is found in the susceptibility fit, indicating imperfect description of the magnetic coupling. Because the molecule contains an inversion center, the coupling to the second cobalt ion, as well as the zero-field splitting of this second cobalt ion must be equivalent and collinear. This then allows the susceptibility to be calculated (red line in Figure 2), where *g*-values of **1** were used. The plot reveals that the maximum in the χT value is calculated at a lower temperature than that found in the experiment. This demonstrates that the interaction is underestimated in the calculation and shows that the description of spin-orbit coupling (leading to ZFS) is better than that of dynamical correlations (leading to *J*). This is partly because only the diagonal elements of the spin-orbit matrix were calculated at perturbational CASPT2 level, and partly due to the diamagnetic substitution of one cobalt ion. For such strong exchange couplings, this diamagnetic substitution of one cobalt is a very rough approximation, because three-center effects to the coupling might play an important role. However, a more accurate treatment of dynamical correlation by, for example, MRCI is not possible because of the size of the system. Moreover, a calculation of the full system without diamagnetic substitution of one cobalt ion is not feasible because it requires a very large active space and the calculation of numerous roots for the SO-coupling step.

An important question is then how the magnetization dynamics is changed going from **1** to **2**. To this end, we carried out ac susceptibility measurements on a powder sample of **2** in zero external magnetic field (Figure 3, Figures S2, S3). We observe a clear, frequency-dependent out-of-phase signal at temperatures up to >25 K. These curves were fit to the standard modified Debye function (Table S4). The $\chi_T - \chi_S$ values agree well with the dc susceptibility (Figure S4), indicating that the entire sample participates in the slow relaxation process. Alpha values of 0.3–0.4 indicate a non-negligible distribution in relaxation times. The relaxation time

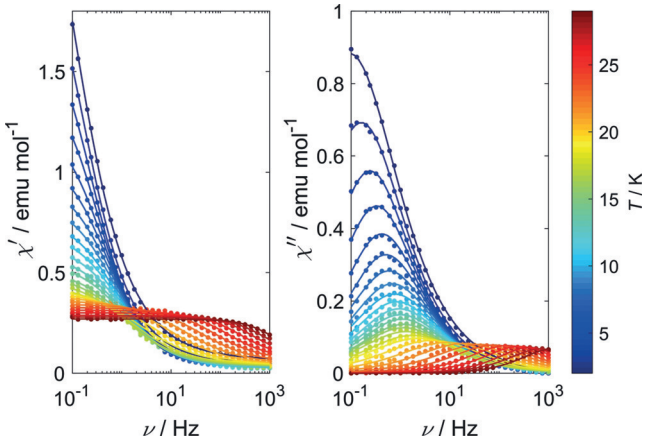

Figure 3. In phase (χ') (left) and out-of-phase (χ'') (right) components of the dynamic susceptibility as a function of frequency of applied magnetic field recorded on a pressed powder sample of **2** in zero external field at different temperatures as indicated by the color scale.

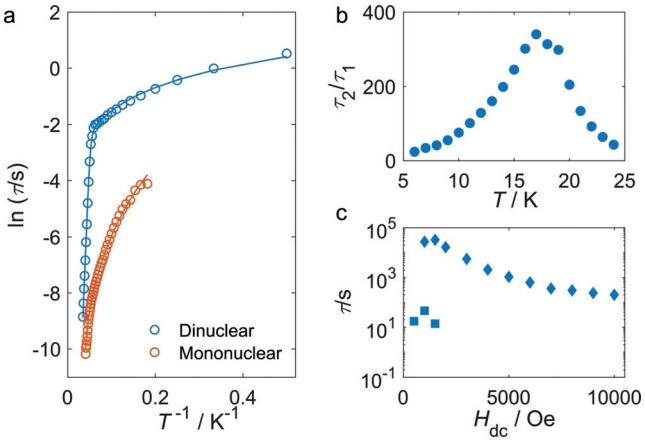

Figure 4. a) Natural logarithm of the relaxation time as a function of inverse temperature for **1** (dark orange symbols), taken from Ref. [10] and **2** (blue symbols). The solid lines are fits to the Equation given in the text. b) Ratio τ_2/τ_1 of the relaxation times of the mononuclear complex **1** (τ_1) and the dinuclear complex **2** (τ_2). c) DC magnetization relaxation times obtained from stretched exponential fits of the magnetization decay for **2**. At low fields, two distinct fast (squares) and slow (diamond) relaxation processes were observed.

τ shown in Figure 4 as an Arrhenius plot of $\ln \tau$ versus T^{-1} decreases by a factor of less than 10 going from 2 to 20 K before decreasing much faster at higher temperatures. The linear dependence in the Arrhenius plot indicates an exponential temperature dependence of the relaxation time at temperatures $T > 20$ K. The temperature dependence of the relaxation time can be fitted very well to a sum of two terms [Eq. (2)]:

$$\tau^{-1} = \tau_0^{-1} \exp(-U_{eff}/kT) + CT^n \qquad (2)$$

The exponential term corresponds to the Orbach relaxation process, in which relaxation proceeds via the excited Kramers doublet. For the exponent in the power law term, many values have been reported, with high values ($n = 7$–9) predicted for the Raman process in extended solids, but lower values of approximately 4 when the vibrations involved are of a local nature.[11] The best fit of the temperature dependence of the relaxation time to Equation (2) gives the following parameter values: $\tau_0 = 2.4(5) \times 10^{-10}$ s, $U_{eff} = 267(3)$ K, $C = 0.9(2)\ s^{-1}\ K^{-n}$, and $n = 1.20(3)$. The effective energy barrier U_{eff} is quite close to the value of $2D$ found from the fit of the dc susceptibility. The very low value of *n* shows that the power law term in Equation (2) cannot be identified as the Raman process. A linear dependence ($n = 1$) of relaxation rate on temperature is expected for the direct process. However, in the absence of an external field, the components of the ground Kramers doublet must be degenerate and the direct process is therefore not expected to be operative. On the other hand, quantum tunneling of the magnetization is not expected to be temperature-dependent. These considerations may change if the hyperfine interaction with the nuclear spin is taken into account (see below). Apart from these considerations, it is clear from Figure 4 that the relaxation times of **2** are much longer than those of **1** at any temperature, and the

ratio of relaxation times reaches a value of approximately 350 at 18 K (Figure 4b). Given that the energy barrier is essentially unchanged going from **1** to **2**, this difference must be due to a suppression of the Raman process that was a main contributor to relaxation of the magnetization in the mononuclear building block **1**.[10] This demonstrates that the aim of increasing relaxation times by incorporation of promising SMM building blocks into a strongly exchange coupled multispin system has been successful.

The field dependence of the relaxation of the magnetization can also be studied by means of magnetic hysteresis measurements (Figure 5). These measurements show a strong

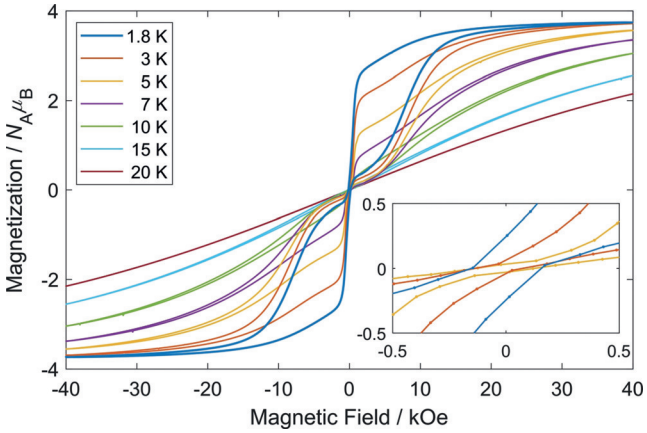

Figure 5. Magnetic hysteresis recorded on a pressed powder sample of **2** at a sweep rate of 20 Oe s^{-1} and different temperatures.

hysteresis up to several Tesla at temperatures up to 15 K, which is quite unusual in cobalt SMMs.[9,10,20–28] Intriguingly, the hysteresis curve is strongly pinched at the waist, and the coercive field is very small, suggesting the occurrence of efficient quantum tunneling. Because of the odd number of unpaired electrons, **2** is a Kramers system, meaning that tunneling cannot be induced by rhombic ZFS. In contrast, the transverse hyperfine interaction of the electron spin with the $I = 7/2$ cobalt nuclear spin can lead to a sizable tunnel splitting. Furthermore, the axial component can lead to level splittings without mixing, which may activate the direct process, leading to a linear temperature dependence of the relaxation time observed in the experiment. An alternative explanation invokes a temperature dependence of the phonon collision rate that is a factor in quantum tunneling.[29] Cobalt hyperfine values of several hundreds of MHz, and clear signatures of hyperfine-induced quantum tunneling have been reported.[27] Intriguingly, manganese(III) has similar hyperfine values,[30] but manganese(III)-based SMMs tend not to display hyperfine-induced relaxation. Single-crystal hysteresis measurements at ultralow temperatures may be able to prove if the hyperfine induces tunneling and/or direct relaxation. The strong hysteresis at fields between 0.1 and 2 T suggests that at these fields, relaxation is much slower than at zero field. Thus, we measured the DC magnetic moment at 1.8 K as a function of time after high-field saturation followed by ramping down the field to the desired end value (Figure S5). Fitting the magnetization decay curves to stretched exponential decay functions yielded the values shown in Figure 4c and Table S5. These data show that indeed the relaxation times increase strongly upon application of an external field and reach values of approximately 32000 s at 1500 Oe. This is much longer than what has been reported for transition-metal complexes with radical ligands (Table S6) and also longer than the 660 s reported for Co-$(C(SiMe_2ONaphthyl)_3)_2$ under the same conditions.[26]

In conclusion, we have shown that by incorporating a highly anisotropic four-coordinate cobalt(II) building block into a radical-bridged dinuclear complex, we have strongly suppressed the Raman process of relaxation of the magnetization leading to a 350-fold increase of the relaxation time of the magnetization. Hyperfine interactions appear to limit the coercivity and thus the magnetic bistability of the complex. We are now studying the exact role of the hyperfine interaction in the magnetization dynamics in this compound.

Acknowledgements

We thank the following for funding: German Science Foundation DFG (SL104/10-1, SA1840/9-1) and the Landesgraduiertenförderung Baden-Württemberg. We thank Samuel Lenz, M.Sc. for help in extracting spin Hamiltonian parameters from the ab initio results.

Conflict of interest

The authors declare no conflict of interest.

Keywords: cobalt · hysteresis · molecular magnetism · Raman process · single-molecule magnet

How to cite: *Angew. Chem. Int. Ed.* **2019**, *58*, 9802–9806
Angew. Chem. **2019**, *131*, 9907–9911

[1] R. Sessoli, D. Gatteschi, A. Caneschi, M. A. Novak, *Nature* **1993**, *365*, 141–143.
[2] A. Baniodeh, N. Magnani, Y. Lan, G. Buth, C. E. Anson, J. Richter, M. Affronte, J. Schnack, A. K. Powell, *NPJ Quantum Mater.* **2018**, *3*, 10.
[3] O. Waldmann, *Inorg. Chem.* **2007**, *46*, 10035–10037.
[4] A. Bencini, D. Gatteschi, *EPR of exchange coupled systems*, Springer, Berlin, **1990**.
[5] C. A. P. Goodwin, F. Ortu, D. Reta, N. F. Chilton, D. P. Mills, *Nature* **2017**, *548*, 439–442.
[6] F.-S. Guo, B. M. Day, Y.-C. Chen, M.-L. Tong, A. Mansikkamäki, R. A. Layfield, *Science* **2018**, *362*, 1400–1403.
[7] F. S. Guo, B. M. Day, Y. C. Chen, M. L. Tong, A. Mansikkamaki, R. A. Layfield, *Angew. Chem. Int. Ed.* **2017**, *56*, 11445–11449; *Angew. Chem.* **2017**, *129*, 11603–11607.
[8] J. M. Zadrozny, D. J. Xiao, M. Atanasov, G. J. Long, F. Grandjean, F. Neese, J. R. Long, *Nat. Chem.* **2013**, *5*, 577–581.
[9] X.-N. Yao, J.-Z. Du, Y.-Q. Zhang, X.-B. Leng, M.-W. Yang, S.-D. Jiang, Z.-X. Wang, Z.-W. Ouyang, L. Deng, B.-W. Wang, S. Gao, *J. Am. Chem. Soc.* **2017**, *139*, 373–380.
[10] Y. Rechkemmer, F. D. Breitgoff, M. van der Meer, M. Atanasov, M. Hakl, M. Orlita, P. Neugebauer, F. Neese, B. Sarkar, J. van Slageren, *Nat. Commun.* **2016**, *7*, 10467.

[11] S. T. Liddle, J. van Slageren, *Chem. Soc. Rev.* **2015**, *44*, 6655 – 6669.
[12] J. D. Rinehart, M. Fang, W. J. Evans, J. R. Long, *J. Am. Chem. Soc.* **2011**, *133*, 14236 – 14239.
[13] J. D. Rinehart, M. Fang, W. J. Evans, J. R. Long, *Nat. Chem.* **2011**, *3*, 538 – 542.
[14] F. Liu, G. Velkos, D. S. Krylov, L. Spree, M. Zalibera, R. Ray, N. A. Samoylova, C.-H. Chen, M. Rosenkranz, S. Schiemenz, F. Ziegs, K. Nenkov, A. Kostanyan, T. Greber, A. U. B. Wolter, M. Richter, B. Büchner, S. M. Avdoshenko, A. A. Popov, *Nat. Commun.* **2019**, *10*, 571.
[15] J. A. DeGayner, I.-R. Jeon, T. D. Harris, *Chem. Sci.* **2015**, *6*, 6639 – 6648.
[16] S. Demir, I.-R. Jeon, J. R. Long, T. D. Harris, *Coord. Chem. Rev.* **2015**, *289 – 290*, 149 – 176.
[17] C. Hua, J. A. DeGayner, T. D. Harris, *Inorg. Chem.* **2019**, https://doi.org/10.1021/acs.inorgchem.1029b00674.
[18] M. Llunell, D. Casanova, J. Cirera, P. Alemany, S. Alvarez, University of Barcelona, Barcelona, **2013**.
[19] P. P. Hallmen, C. Köppl, G. Rauhut, H. Stoll, J. van Slageren, *J. Chem. Phys.* **2017**, *147*, 164101.
[20] E. C. Yang, D. N. Hendrickson, W. Wernsdorfer, M. Nakano, L. N. Zakharov, R. D. Sommer, A. L. Rheingold, M. Ledezma-Gairaud, G. Christou, *J. Appl. Phys.* **2002**, *91*, 7382 – 7384.
[21] A. Ferguson, A. Parkin, J. Sanchez-Benitez, K. Kamenev, W. Wernsdorfer, M. Murrie, *Chem. Commun.* **2007**, 3473 – 3475.
[22] D. Wu, D. Guo, Y. Song, W. Huang, C. Duan, Q. Meng, O. Sato, *Inorg. Chem.* **2009**, *48*, 854 – 860.
[23] S. J. Langley, M. Helliwell, R. Sessoli, P. Rosa, W. Wernsdorfer, R. E. P. Winpenny, *Chem. Commun.* **2005**, 5029.
[24] K. W. Galloway, A. M. Whyte, W. Wernsdorfer, J. Sanchez-Benitez, K. V. Kamenev, A. Parkin, R. D. Peacock, M. Murrie, *Inorg. Chem.* **2008**, *47*, 7438 – 7442.
[25] D. Tu, D. Shao, H. Yan, C. Lu, *Chem. Commun.* **2016**, *52*, 14326 – 14329.
[26] P. C. Bunting, M. Atanasov, E. Damgaard-Møller, M. Perfetti, I. Crassee, M. Orlita, J. Overgaard, J. van Slageren, F. Neese, J. R. Long, *Science* **2018**, *362*, eaat7319.
[27] S. Vaidya, S. Tewary, S. K. Singh, S. K. Langley, K. S. Murray, Y. Lan, W. Wernsdorfer, G. Rajaraman, M. Shanmugam, *Inorg. Chem.* **2016**, *55*, 9564 – 9578.
[28] X. Ma, E. A. Suturina, S. De, P. Négrier, M. Rouzières, R. Clérac, P. Dechambenoit, *Angew. Chem. Int. Ed.* **2018**, *57*, 7841 – 7845; *Angew. Chem.* **2018**, *130*, 7967 – 7971.
[29] Y.-S. Ding, K.-X. Yu, D. Reta, F. Ortu, R. E. P. Winpenny, Y.-Z. Zheng, N. F. Chilton, *Nat. Commun.* **2018**, *9*, 3134.
[30] I. Krivokapic, C. Noble, S. Klitgaard, P. Tregenna-Piggott, H. Weihe, A.-L. Barra, *Angew. Chem. Int. Ed.* **2005**, *44*, 3613 – 3616; *Angew. Chem.* **2005**, *117*, 3679 – 3682.
[31] CCDC 1877351 contains the supplementary crystallographic data for this paper. These data can be obtained free of charge from The Cambridge Crystallographic Data Centre

Manuscript received: April 15, 2019
Accepted manuscript online: May 3, 2019
Version of record online: June 6, 2019

